


Plasmonic Time Crystals

Joshua Feinberg¹, David E. Fernandes², Boris Shapiro³, and Mário G. Silveirinha²

¹*Department of Physics and Haifa Center for Physics and Astrophysics, University of Haifa, Haifa 3498838, Israel*

²*University of Lisbon and Instituto de Telecomunicações, Avenida Rovisco Pais 1, Lisboa 1049-001, Portugal*

³*Department of Physics, Technion, Israel Institute of Technology, Haifa 32000, Israel*

 (Received 31 July 2024; revised 4 March 2025; accepted 1 April 2025; published 6 May 2025)

We study plasmonic time crystals, an extension of dielectric-based photonic time crystals to plasmonic media. We demonstrate that such systems may amplify both longitudinal and transverse modes. In particular, we show that plasmonic time crystals support “collective resonances” of longitudinal modes, which occur independent of the wave vector k , even in the presence of significant dissipation. These resonances originate from the coupling between the positive- and negative-frequency branches of the plasmonic dispersion relation of the unmodulated system and from the divergence of the density of states near the plasma (ϵ -near-zero) frequency ω_p . The strongest resonance arises at a modulation frequency $\Omega = 2\omega_p$, corresponding to a direct interband transition. We demonstrate these resonances for various periodic modulation profiles and provide a generic perturbative formula for resonance widths in the weak modulation limit. Furthermore, we propose transparent conducting oxides as promising platforms for realizing plasmonic time crystals, as they enable significant modulation of the electron effective mass while maintaining moderate dissipation levels. Our findings provide new insights into leveraging time-modulated plasmonic media to enhance optical gain and control wave dynamics at the nanoscale.

DOI: [10.1103/PhysRevLett.134.183801](https://doi.org/10.1103/PhysRevLett.134.183801)

Introduction—Temporal modulation of a material amounts to changing in time some parameters of the material. In this way, a new artificial (or meta) material is created, with new and useful properties [1,2]. In particular, if the dielectric permittivity ϵ of a material undergoes periodic modulation, then a photonic time crystal (PTC) is produced [3]. A PTC can amplify electromagnetic waves with wave numbers k lying in its k band gaps [4]. k bands are analogous to the frequency bands in a spatial photonic crystal.

Generally, the concept of temporal modulation applies to arbitrary time dependence $\epsilon(t)$. For instance, the behavior of an electromagnetic wave under sudden change of ϵ at some instant $t = t_0$ has been considered already in 1958 [5]. The case of $\epsilon(t)$ being a random function of time has been studied recently in [3,6]. By now, temporal modulation of materials has become a broad and active field of research with many theoretical [3–28] and some experimental [29–32] works.

A few previous works have investigated some particular forms of dispersive time crystals, focusing mainly on transverse waves [18,33–38]. Let us also mention possible amplification of localized plasmons [39], as well as surface plasmons [40]. This ongoing work on parametric amplification in various types of PTCs must be distinguished from the old work on parametric resonances and instabilities in gaseous plasmas (see, e.g., [41]).

In this Letter, we extend the study of PTCs to longitudinal excitations of an electron gas. In conventional

PTCs, which rely on permittivity modulation in dielectric materials, both the modulation depth and frequency face stringent constraints. Specifically, both must be sufficiently large to produce observable k gaps and significant amplification rates. Here, we demonstrate that “plasmonic time crystals” (PLTCs) serve as exceptional platforms for generating optical gain. More precisely, we show the possibility of achieving a collective resonance that can significantly enhance parametric gain. This collective resonance arises from the coupling of plasmons with positive and negative frequencies and is characterized by a diverging density of states. Such a resonance can occur for any mode with a k -independent dispersion relation. In particular, it applies to longitudinal plasmons, whose temporal modulation, to the best of our knowledge, has not been previously studied.

Infinite band gaps for transverse waves were analyzed in a recent work [38]. Here, we show that, unlike the transverse resonant case [38], longitudinal waves support a collective resonance even in the presence of dissipation. Thus, for a longitudinal plasmon, a very wide (theoretically “infinite”) k gap emerges naturally, leaving only the challenge of ensuring a substantial amplification rate. We also note that the temporal modulation of longitudinal optical phonons was analyzed in [42] in the context of the interaction of a point charge with a time-modulated medium.

Physical model—We consider a conducting material whose electric response is determined by both bound and free electrons. We assume that the response of the

conducting material is modulated in time via a nonlinear process driven by optical pumping. In this context, transparent conducting oxides (TCOs) have recently attracted considerable attention [43–49], as it has been demonstrated that optical pumping can induce strong refractive index modulations in the near-zero permittivity (ENZ) regime [50,51]. Moreover, recent studies have shown that time interfaces as short as a single optical cycle can also be generated with such a modulation scheme [49].

The nonlinearity of ENZ materials excited below the band gap is governed primarily by the modulation of their absorption properties and by the modulation of the effective mass of free electrons [52]. In a plasma subjected to optical pumping, a significant fraction of conduction electrons is excited to higher energy states within the conduction band, forming a population of “hot electrons.” Because of the nonparabolicity of the conduction band, these hot electrons may experience an effective mass m^* that differs from its equilibrium value. Furthermore, the increased energy of the hot electron population can enhance the probability of lattice collisions, rendering the collision frequency ν a time-dependent parameter [52].

In this Letter, we concentrate on homogeneous and isotropic media. Consequently, electromagnetic excitations in our system are either longitudinal or transverse. In what follows, we shall focus mainly on longitudinal plasmons. (Transverse plasmons will be discussed mainly in comparison with longitudinal plasmons.)

Longitudinal plasmons—For this type of excitation, the magnetic field in the material is negligible, and the electron displacement away from equilibrium oscillates along the same direction as the electric field gradient in space, as we show below. In order to derive the equation governing the dynamics of (volume) longitudinal plasmons in a material [53,54], consider some volume of the electron gas displaced by an amount \mathbf{u} relative to the neutralizing ionic background, as illustrated in Fig. 1(a). (Note that the displaced electrons can belong to an arbitrary region within the material.) By applying Newton’s law to the displaced electrons, we obtain $M(d^2\mathbf{u}/dt^2) + M\nu(d\mathbf{u}/dt) = Q\mathbf{E}$, where $M = m^*N_e$ is the total effective mass of the displaced electrons, $Q = -eN_e$ is their total charge, and N_e is the number of displaced electrons. The term proportional to $\nu(d\mathbf{u}/dt)$ accounts for dissipation due to collisions.

The electric field \mathbf{E} acting on the displaced electrons is obviously the field generated by the excess of negative charge in a layer of thickness u and by the corresponding layer of uncompensated positive ionic charge of the same thickness [see Fig. 1(a)]. Elementary electromagnetic analysis then yields $\mathbf{E} = e(4\pi n_0\mathbf{u}/\epsilon)$, where n_0 is the density of free electrons, and $\epsilon = 1 + 4\pi\chi_e$ represents the permittivity of the background with the contribution from bound electrons described by the electric susceptibility χ_e . (We adopt Gaussian units.) This relation essentially means

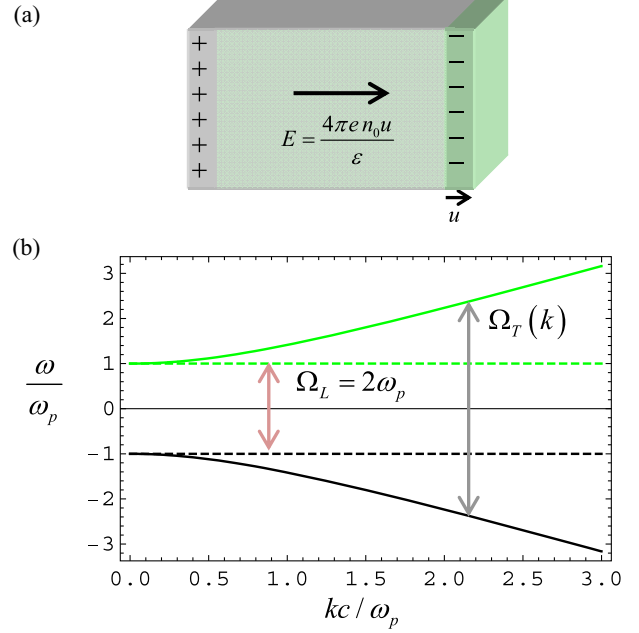


FIG. 1. (a) Illustration of the displacement of a region of the electron gas. The displacement generates a region of thickness u with an excess of negative charge and a corresponding region of equal thickness with positive charge due to the uncompensated ionic background. (b) Band structure of the static dispersive crystal, showing both positive- and negative-frequency bands. The arrows indicate possible interband transitions.

that the total electric displacement field $\mathbf{D} = \epsilon\mathbf{E} - 4\pi en_0\mathbf{u} = 0$ vanishes throughout the plasma medium.

Upon substituting the relation between \mathbf{E} and \mathbf{u} in the equation of motion, we find that the electron displacement obeys the equation

$$m^*(t) \frac{d^2\mathbf{u}}{dt^2} + m^*(t)\nu(t) \frac{d\mathbf{u}}{dt} + e^2 \frac{4\pi n_0}{\epsilon(t)} \mathbf{u} = 0. \quad (1)$$

We have incorporated the effect of optical pumping by allowing the effective mass and collision frequency to vary with time. Furthermore, for completeness, we also consider the impact of optical pumping on the susceptibility of the bound electrons, as in conventional nonlinear optics. As a result, optical pumping can also modulate the permittivity ϵ of the background, although this effect is typically less significant than the modulation of the free electron response.

In Supplemental Material [55] we provide a more formal derivation of (1) governing longitudinal plasmons by considering Maxwell’s equations coupled with a transport equation with time-varying coefficients.

For simplicity, in the main text, we neglect the modulation of the bound electrons permittivity, and thus set ϵ to its unmodulated equilibrium value ϵ_0 . (Modulation of ϵ is qualitatively similar to modulation of the effective mass [55].) Furthermore, we also assume that ν is time

independent, treating it as a time-averaged collision frequency. The theoretical justification for this approximation is provided in Supplemental Material [55]. Under these assumptions, Eq. (1) can be rewritten as

$$\frac{d^2 f}{dt^2} + \omega_p^2 [1 + \delta_m(t)] f + \nu \frac{df}{dt} = 0, \quad (2)$$

where f is any component of the displacement vector \mathbf{u} . Here, ω_p is the plasma frequency of the unmodulated (equilibrium) system, defined as $\omega_p^2 = 4\pi e^2 n_0 / m_0^* \epsilon_0$, where m_0^* is the effective mass of electrons in the unmodulated system and where we have parametrized the modulated effective mass as $1/m^* = [1 + \delta_m(t)]/m_0^*$. We shall refer to the dimensionless fractional quantity $\delta_m(t)$ as the modulation depth (or modulation profile).

Equation (2) describes a damped parametric oscillator [57]. The first-order damping term in (2) may be eliminated by redefining $f = e^{-\nu t/2} g$. The resulting equation for g is

$$\frac{d^2 g}{dt^2} + \omega_p^2 \left(1 - \frac{\nu^2}{4\omega_p^2} + \delta_m(t) \right) g = 0. \quad (3)$$

Since our plasma is spatially homogeneous, it suffices to consider waves with a spatial dependence of the form $\sim e^{i\mathbf{k} \cdot \mathbf{r}}$. A distinctive feature of Eq. (2) is that it does not involve the wave number k . This property is unique to longitudinal plasmons, owing to their intrinsic k -independent dispersion relation, $\omega = \pm \omega_p$ [see the dashed lines in Fig. 1(b)]. Such a dispersion implies that, once time modulation is switched on, the function $f(t)$ —along with all other relevant quantities—can undergo exponential growth simultaneously for *all* k modes. This collective resonance enhances the interaction between the plasma and the optical pump, leading to strong parametric amplification, as we elaborate below.

In particular, it is important to emphasize that, under periodic modulation $\delta_m(t)$ with modulation frequency Ω , all k modes of a longitudinal plasmon excitation are amplified at the same frequency Ω_{ampl} . This is the collective longitudinal resonance alluded to in the Abstract. The overall scale of Ω_{ampl} is essentially fixed by the two dimensionful quantities in (2), namely, ω_p and ν [58]. The latter, in turn, determine the location of the ENZ resonance $\epsilon(\omega) = 0$ (on the unmodulated permittivity), even in the presence of dissipation [59]. In contrast, the related concept discussed in Ref. [38] relies on the condition $\epsilon(\omega) = \infty$, which in principle is more sensitive to dissipation effects.

Under periodic modulation profile $\delta_m(t)$, the two Floquet-type fundamental solutions of (2) are of the form [55,60–62] $f_{1,2}(t) = e^{-i\omega_{1,2}t} u_{1,2}(t)$, where $\omega_{1,2}$ are the two fundamental frequencies, and $u_{1,2}(t)$ are periodic functions with period $T = 2\pi/\Omega$ [55]. The fundamental frequencies

$\omega_{1,2} = \omega'_{1,2} + i\omega''_{1,2}$ are typically complex. Thus, if (at most) one of the imaginary parts $\omega''_{1,2}$ is positive, the corresponding Floquet solution will grow as function of time, rendering the system unstable.

The eigenfrequencies $\omega_{1,2}$ depend on the modulation frequency Ω and on the parameters controlling the (dimensionless) modulation profile $\delta_m(t)$. This parameter space is split into regions of stability and instability, separated by borderlines. In regions of stability, oscillations of $f(t)$ are bounded, while in regions of instability $f(t)$ exhibits resonant behavior, with unbounded oscillations. These general statements are demonstrated succinctly by the following two examples:

Harmonic modulation: $\delta_m(t) = \delta_{mM} \cos \Omega t$. In this case (and in the absence of losses), Eq. (2) reduces to the famous Mathieu equation [60–64], which exhibits rich structure of stability and instability regions in the space of parameters Ω/ω_p and δ_{mM} . In particular, for $\Omega = 2\omega_p$, it is well known that the amplitude of oscillations grows exponentially approximately as $\exp(\delta_{mM}\omega_p t/4)$. In our problem, this instability can be interpreted as a collective resonance (i.e., for all values of the wave number k) due to the interband transitions between the two branches $\pm\omega_p$ of the static (unmodulated) crystal [see Fig. 1(a)] [35,65]. This instability persists also when Ω is slightly detuned away from $2\omega_p$, albeit with a smaller growth exponent [57] $\omega'' \simeq (\omega_p/4) \sqrt{\delta_{mM}^2 - 16\Delta^2}$, where $\Delta = (\Omega/2\omega_p) - 1$ is the detuning parameter.

The width of the instability region around $\Omega = 2\omega_p$ is determined by reality of ω'' . In particular, this means that there is a minimal threshold value of $\delta_{mM}^{\text{Th}} = 4|\Delta|$ required to induce instability. Similar but weaker instabilities occur also at modulation frequencies around $\Omega_n = 2\omega_p/n$ with integer n [57]. Finally, such exponential growth, albeit with smaller amplification rate $\omega''(\nu) \simeq \omega''(0) - \nu/2$, persists also for sufficiently small ν , as should be clear from the argument leading to (3) [57].

In particular, it follows that, for a sinusoidal-type modulation of the effective mass, the minimum modulation depth required to overcome losses (at resonance) is approximately $\delta_{mM} \approx 2\nu/\omega_p$. The ratio ν/ω_p can be related to the imaginary part of the complex permittivity, $\epsilon''(\omega)$, evaluated at the ENZ frequency via $(\nu/\omega_p) \approx (\epsilon''_{\text{ENZ}}/\epsilon)$, where ϵ is the permittivity due to bound electrons. Consequently, the required modulation depth is $\delta_{mM} \approx 2(\epsilon''_{\text{ENZ}}/\epsilon)$. For typical TCOs, $\epsilon \sim 3\text{--}4$ and $\epsilon''_{\text{ENZ}} \sim 0.2\text{--}0.5$ [44,46]. According to Ref. [52], for TCOs δ_{mM} varies linearly with the pump intensity and can be as large as 0.2. Therefore, while challenging, attaining the required modulation depth for optical gain appears feasible in these materials.

Periodic piecewise constant modulation: In this case, in its simplest form, $\delta_m(t)$ assumes one constant value δ_{m1} during the first part $0 \leq t < \tau$ of the modulation period

and another constant value δ_{m2} during its remaining part $\tau \leq t < T$ [60,61]. For concreteness, let us focus on the modulation

$$\delta_m(t) = \delta_{mM} \text{sgn}(\sin(\Omega t)), \quad (4)$$

which flips sign at the middle of the modulation period. Here, as in the case of Mathieu's equation, one obtains a rich chart of stability and instability regions in the plane of parameters Ω/ω_p and δ_{mM} [60,61]. In particular, for weak modulation amplitude δ_{mM} (and in the absence of dissipation $\nu = 0$), we find an infinite family of resonances analogous to the aforementioned resonance of the Mathieu equation, centered at modulation frequencies $\Omega_n^{\text{odd}} = 2\pi/T = 2\omega_p/(2n+1)$ with integer n and with growth exponents [55]

$$\omega'' = \omega_p \sqrt{\frac{\delta_{mM}^2}{[(2n+1)\pi]^2} - \Delta^2}, \quad (5)$$

where $\Delta = \Omega/\Omega_n^{\text{odd}} - 1$ is the detuning parameter. Thus, at the center of the resonance ($\Delta = 0$), $\omega''_{\text{Res}} = \omega_p \delta_{mM}/(2n+1)\pi$ is linear in δ_{mM} and is therefore of leading order in perturbation theory. Furthermore, similar to the Mathieu

case, detuning the modulation frequency away from the resonance requires a threshold value $\delta_{mM}^{\text{Th}} = (2n+1)\pi|\Delta|$ of the modulation amplitude to induce instability with diminished ω'' .

In addition to this family of “linear resonances,” we find that there is yet another family of weaker resonances centered in the vicinity of modulation frequencies $\Omega_n^{\text{even}} = 2\omega_p/2n = \omega_p/n$ with integer n , with growth exponents [55]

$$\omega'' = \omega_p \sqrt{\left(\frac{\delta_{mM}^2}{4}\right)^2 - \left(\Delta + \frac{\delta_{mM}^2}{8}\right)^2}, \quad (6)$$

where $\Delta = \Omega/\Omega_n^{\text{even}} - 1$ is the detuning parameter away from Ω_n^{even} . In contrast to (5), the centers of these resonances (i.e., maximal instability) occur at modulation frequencies $\Omega_n^{\text{Res}} = \Omega_n^{\text{even}}(1 - \delta_{mM}^2/8)$, which depend quadratically on δ_{mM} . Furthermore, at $\Omega = \Omega_n^{\text{Res}}$, all these resonances share an “ n -independent” common growth exponent $\omega''_{\text{Res}} = \omega_p \delta_{mM}^2/4$, quadratic in δ_{mM} , and therefore of higher order in perturbation theory.

The predictions of (5) and (6) are compared against numerical simulation of the piecewise constant modulation in Figs. 2(ai)–2(aiii), showing excellent agreement.

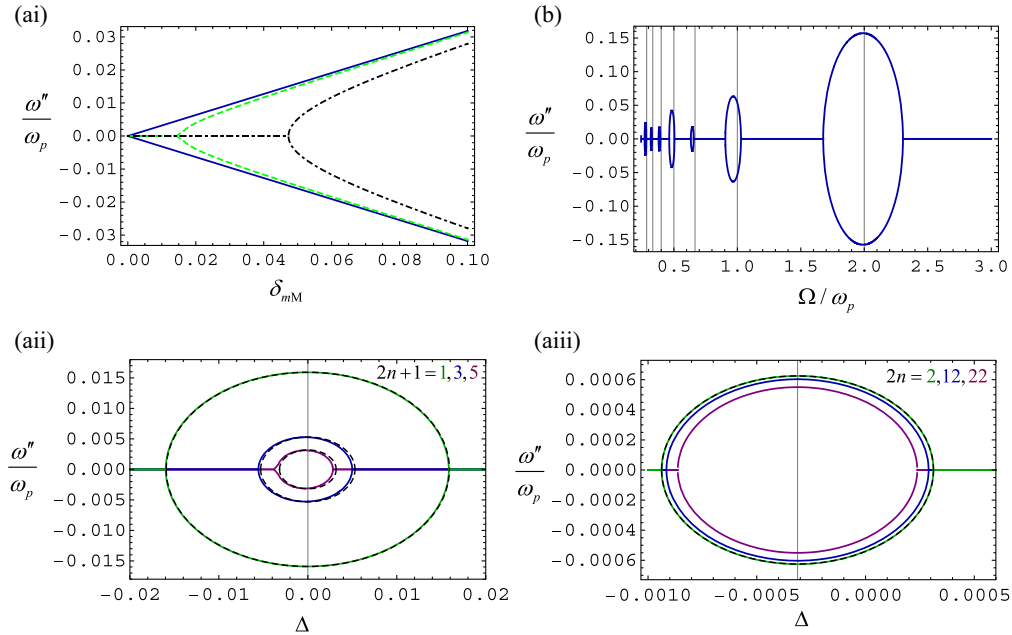


FIG. 2. (ai) ω'' as a function of the (weak) modulation strength for (i) $\Omega = 2\omega_p$ (blue solid lines), (ii) $\Omega = (2 \pm 0.01)\omega_p$ (green dashed lines), and (iii) $\Omega = (2 \pm 0.03)\omega_p$ (black dotted lines). (aii) ω'' as a function of the detuning parameter Δ for fixed weak modulation amplitude $\delta_{mM} = 0.05$ for the first three odd resonances ($2n+1 = 1, 3, 5$) in (5). The dashed curves are the analytic predictions. The three resonances are centered at $\Delta = 0$ and the growth rate becomes smaller as n increases. (aiii) The same as in (aii) with $\delta_{mM} = 0.05$ for the even resonances $2n = 2, 12, 22$ in (6). Note the smaller vertical scale compared to the previous case. The three displayed resonances are in good agreement with the n -independent prediction of (6), despite the large disparity of chosen values for n . Evidently, these three resonances are centered around a negative value of Δ consistent with $-\delta_{mM}^2/8$ as predicted in (6). (b) ω'' as a function of the modulation frequency Ω for fixed strong modulation amplitude $\delta_{mM} = 0.5$. The vertical grid lines mark the resonant modulation frequencies $\Omega = 2\omega_p/m$ with $m = 1, 2, \dots, 7$ for the weak modulation case.

In Fig. 2(b) we show numerical results for the growth rates ω'' of resonances arising at fixed strong modulation amplitude $\delta_{mM} = 0.5$ as function of the modulation frequency Ω . The general pattern of resonances at weak modulation amplitudes, summarized in (5) and (6), is clearly preserved, up to some amount of bounded shifts in resonance frequencies. However, as can be clearly seen in Fig. 2, at strong modulation amplitude, the strength of the even resonances of (6) can become comparable to, or even surpass, the odd resonances of (5). Furthermore, under strong modulation, the gain rate no longer scales linearly with δ_{mM} . Hence, the weak modulation evaluation of the gain typically underestimates the actual gain, potentially facilitating a practical realization.

In Supplemental Material we give a simple perturbative derivation of the growth rate ω'' of linear resonances (at zero detuning $\Delta = 0$ and in the absence of losses $\nu = 0$) for an arbitrary weak periodic modulation profile $\delta_m(t)$ in (2) [55]. Our analysis confirms that the instabilities generally occur when the modulation frequency Ω is commensurate with the gap width $2\omega_p$ of the unmodulated longitudinal plasmons, such that $2\omega_p/\Omega = n$, with integer n . Specifically, the growth rate of the n th resonance is governed by the n th Fourier coefficient of $\delta_m(t) = \sum_{l=1}^{\infty} (c_l \exp(il\Omega t) + c_l^* \exp(-il\Omega t))$, such that

$$\omega''_n = \frac{\omega_p |c_n|}{2}. \quad (7)$$

This result is linear in c_n , and therefore in δ_m , because it arises from first-order perturbation theory. The above formula includes as particular cases the harmonic (Mathieu) modulation and the piecewise constant modulation, discussed previously [55]. Moreover, in Supplemental Material [55], we demonstrate that, for a given peak modulation depth δ_{mM} , the optimal modulation profile that maximizes optical gain corresponds to a piecewise constant modulation.

Transverse waves—We shall now briefly consider temporal modulation of transverse waves [18,33–37], mainly in order to compare it against that of longitudinal plasmons. We shall assume in this section that the material dissipation is negligible ($\nu = 0$). For transverse waves, the oscillations of free electrons occur along a direction perpendicular to the spatial field gradients, i.e., perpendicular to the wave vector \mathbf{k} . A detailed analysis presented in Supplemental Material shows that the time dynamics of transverse waves is governed by [55]

$$\frac{d^2 \mathbf{D}_b}{dt^2} + \omega_T^2 \left[1 + \frac{\omega_p^2}{\omega_T^2} \delta_m(t) \right] \mathbf{D}_b = 0, \quad (8)$$

where $\omega_T^2 = (c^2 k^2 / \epsilon_0) + \omega_p^2$ is (k -dependent) transverse wave dispersion, and $\mathbf{D}_b = \epsilon \mathbf{E}$, where \mathbf{E} is the electric field. The plane wave spatial variation $\sim e^{i\mathbf{k} \cdot \mathbf{r}}$ of the fields is implicit. Furthermore, analogous to the case of longitudinal

plasmons, in the following we suppose that ϵ remains time independent.

Equation (8) is qualitatively similar in form to (2) (with $\nu = 0$). It coincides with the latter at $k = 0$ and therefore describes a parametric oscillator, as in the case of longitudinal plasmons. Evidently, we can translate the entire previous discussion of resonances in modulated longitudinal plasmons to transverse plasmons, simply by replacing ω_p in the appropriate places by ω_T and by rescaling the modulation amplitude $\delta_m(t)$ by a factor ω_p^2/ω_T^2 . Thus, compared to the longitudinal case, the modulation amplitude is effectively reduced and the resonance frequency of the system is increased. Stability regions in the parameter space pertaining to modulated longitudinal plasmons become k bands of the transverse PLTC, while regions of instability correspond to gaps.

Importantly, the resonances associated with Eq. (8) arise separately for each wave number k , in contrast to the collective, k -independent nature of resonances in modulated longitudinal plasmons. As a result, the resonances associated with transverse waves are weaker, both due to the reduced modulation depth and because they remain isolated from one another.

For example, in the case of piecewise constant modulation (4), we see from (5), pertaining to longitudinal plasmons, that there will be resonances of the transverse plasmon at modulation frequency $\Omega_{n,T}^{\text{odd}} = 2\omega_T/(2n+1)$ with integer n and growth exponents $\omega'' = \omega_T \sqrt{[\omega_p^2 \delta_{mM}/(2n+1)\pi\omega_T^2]^2 - \Delta^2}$, in which $\Delta = \Omega/\Omega_{n,T}^{\text{odd}} - 1$ is the detuning parameter. Analogous results exist obviously also for the weaker longitudinal resonances (6). A numerical example is reported in Supplemental Material [55].

Conclusions—In this Letter, we have carried out a comprehensive study of plasmonic time crystals, demonstrating that these platforms support both longitudinal and transverse modes. We have shown that, under periodic time modulation, these systems function as parametric oscillators, and we have analyzed their stability properties across a broad range of parameters.

Notably, the resonance of longitudinal modes is independent of the wave vector \mathbf{k} , even in the presence of significant dissipation, enabling a collective resonance that can be leveraged to achieve optical amplification. The strongest parametric instabilities arise from interband transitions at modulation frequency $\Omega = 2\omega_p$. In particular, we have proposed that TCOs are well suited for realizing plasmonic time crystals, as they allow for significant modulation of the electron effective mass while maintaining a moderate dissipation level [43–49].

In contrast, transverse resonances depend on the wave vector \mathbf{k} of propagating waves and remain isolated from one another, limiting their capacity for collective amplification. Our findings pave the way for the exploration of

plasmonic time crystals as a platform for tunable optical amplification in nanophotonics.

Acknowledgments—B. S. is indebted to Remi Carminati for useful discussions at the early stage of this work. B. S. is also grateful for the hospitality extended to him during his visit to the University of Lisbon in October 2022, where this project was initiated. J. F. is supported in part by Grant No. 2022158 from the United States-Israel Binational Science Foundation (BSF), Jerusalem, Israel. D. E. F. acknowledges financial support by IT-Lisbon and FCT under a research contract Ref. CEECINST/00058/2021/CP2816/CT0003 and Grant DOI 10.54499/CEECINST/00058/2021/CP2816/CT0003. M. S. is partially supported by the IET, by the Simons Foundation under Award No. 733700 (Simons Collaboration in Mathematics and Physics, Harnessing Universal Symmetry Concepts for Extreme Wave Phenomena), and by FCT/MECI through national funds and when applicable co-funded EU funds under UID/50008: Instituto de Telecomunicações, and under project 2022.06797.PTDC.

- [1] C. Caloz and Z.-L. Deck-Léger, Spacetime metamaterials—Part I: General concepts, *IEEE Trans. Antennas Propag.* **68**, 1569 (2020); Spacetime metamaterials—Part II: Theory and Applications, *IEEE Trans. Antennas Propag.* **68**, 1583 (2020).
- [2] E. Galiffi, R. Tirole, S. Yin, H. Li, S. Vezzoli, P. A. Huidobro, M. G. Silveirinha, R. Sapienza, A. Alù, and J. B. Pendry, Photonics of time-varying media, *Adv. Photonics* **4**, 014002 (2022).
- [3] Y. Sharabi, E. Lustig, and M. Segev, Disordered photonic time crystals, *Phys. Rev. Lett.* **126**, 163902 (2021).
- [4] J. R. Zurita-Sánchez, P. Halevi, and J. C. Cervantes-González, Reflection and transmission of a wave incident on a slab with a time-periodic dielectric function, *Phys. Rev. A* **79**, 053821 (2009).
- [5] F. Morgenthaler, Velocity modulation of electromagnetic waves, *IRE Trans. Microwave Theory Tech.* **6**, 167 (1958).
- [6] R. Carminati, H. Chen, R. Pierrat, and B. Shapiro, Universal statistics of waves in a random time-varying medium, *Phys. Rev. Lett.* **127**, 094101 (2021).
- [7] A. Akbarzadeh, N. Chamanara, and C. Caloz, Inverse prism based on temporal discontinuity and spatial dispersion, *Opt. Lett.* **43**, 3297 (2018).
- [8] V. Pacheco-Peña and N. Engheta, Temporal aiming, *Light Sci. Appl.* **9**, 129 (2020).
- [9] J. Xu, W. Mai, and D. H. Werner, Complete polarization conversion using anisotropic temporal slabs, *Opt. Lett.* **46**, 1373 (2021).
- [10] H. Li, S. Yin, E. Galiffi, and A. Alù, Temporal parity-time symmetry for extreme energy transformations, *Phys. Rev. Lett.* **127**, 153903 (2021).
- [11] H. Li, S. Yin, and A. Alù, Nonreciprocity and Faraday rotation at time interfaces, *Phys. Rev. Lett.* **128**, 173901 (2022).
- [12] A. Dikopoltsev, Y. Sharabi, M. Lyubarov, Y. Lumer, S. Tsesses, E. Lustig, I. Kaminer, and M. Segev, Light emission by free electrons in photonic time-crystals, *Proc. Natl. Acad. Sci. U.S.A.* **119**, e2119705119 (2022).
- [13] N. V. Budko, Electromagnetic radiation in a time-varying background medium, *Phys. Rev. A* **80**, 053817 (2009).
- [14] M. Lyubarov, Y. Lumer, A. Dikopoltsev, E. Lustig, Y. Sharabi, and M. Segev, Amplified emission and lasing in photonic time crystals, *Science* **377**, 425 (2022).
- [15] E. Lustig, Y. Sharabi, and M. Segev, Topological aspects of photonic time crystals, *Optica* **5**, 1390 (2018).
- [16] M. J. Mencagli, D. L. Sounas, M. Fink, and N. Engheta, Static-to-dynamic field conversion with time-varying media, *Phys. Rev. B* **105**, 144301 (2022).
- [17] H. Li, S. Yin, H. He, J. Xu, A. Alù, and B. Shapiro, Stationary charge radiation in anisotropic photonic time crystals, *Phys. Rev. Lett.* **130**, 093803 (2023).
- [18] D. M. Solís, R. Kastner, and N. Engheta, Time-varying materials in the presence of dispersion: Plane-wave propagation in a Lorentzian medium with temporal discontinuity, *Photonics Res.* **9**, 1842 (2021).
- [19] D. M. Solís and N. Engheta, Functional analysis of the polarization response in linear time-varying media: A generalization of the Kramers-Kronig relations, *Phys. Rev. B* **103**, 144303 (2021).
- [20] Z. Hayran, J. B. Khurgin, and F. Monticone, $\hbar\omega$ versus $\hbar k$: Dispersion and energy constraints on time-varying photonic materials and time crystals, *Opt. Mater. Express* **12**, 3904 (2022).
- [21] J. Sloan, N. Rivera, J. D. Joannopoulos, and M. Soljacic, Optical properties of dispersive time-dependent materials, *ACS Photonics* **11**, 950 (2024).
- [22] S. A. R. Horsley, E. Galiffi, and Y.-T. Wang, Eigenpulses of dispersive time-varying media, *Phys. Rev. Lett.* **130**, 203803 (2023).
- [23] G. Ptitcyn *et al.*, Floquet-Mie theory for time-varying dispersive spheres, *Laser Photonics Rev.* **17**, 2100683 (2023).
- [24] M. M. Dimitrijevic and B. V. Stanic, EMW transformation in suddenly created two-component magnetized plasma, *IEEE Trans. Plasma Sci.* **23**, 422 (1995).
- [25] D. Holberg and K. Kunz, Parametric properties of fields in a slab of time-varying permittivity, *IEEE Trans. Antennas Propag.* **14**, 183 (1966).
- [26] F. R. Prudêncio and M. G. Silveirinha, Synthetic axion response with spacetime crystals, *Phys. Rev. Appl.* **19**, 024031 (2023).
- [27] F. R. Prudêncio and M. G. Silveirinha, Replicating physical motion with Minkowskian isorefractive spacetime crystals, *Nanophotonics* **12**, 3007 (2023).
- [28] J. T. Mendonça, *Theory of Photon Acceleration* (IOP Publishing, Bristol, 2001).
- [29] V. Bacot, M. Labousse, A. Eddi, M. Fink, and E. Fort, Time reversal and holography with spacetime transformations, *Nat. Phys.* **12**, 972 (2016).
- [30] V. Bacot, G. Durey, A. Eddi, M. Fink, and E. Fort, Phase-conjugate mirror for water waves driven by the Faraday instability, *Proc. Natl. Acad. Sci. U.S.A.* **116**, 8809 (2019).
- [31] H. Moussa, G. Xu, S. Yin, E. Galiffi, Y. Radi, and A. Alù, Observation of temporal reflections and broadband

- frequency translations at photonic time-interfaces, *Nat. Phys.* **19**, 863 (2023).
- [32] B. Apffel, S. Wildeman, A. Eddi, and E. Fort, Experimental implementation of wave propagation in disordered time-varying media, *Phys. Rev. Lett.* **128**, 094503 (2022).
- [33] H. He, S. Zhang, J. Qi, F. Bo, and H. Li, Faraday rotation in nonreciprocal photonic time-crystals, *Appl. Phys. Lett.* **122**, 051703 (2023).
- [34] J. C. Serra and M. G. Silveirinha, Homogenization of dispersive spacetime crystals: Anomalous dispersion and negative stored energy, *Phys. Rev. B* **108**, 035119 (2023).
- [35] J. C. Serra, E. Galiffi, P. A. Huidobro, J. B. Pendry, and M. G. Silveirinha, Particle-hole instabilities in photonic time-varying systems, *Opt. Mater. Express* **14**, 1459 (2024).
- [36] F. Feng, N. Wang, and G. P. Wang, Temporal transfer matrix method for Lorentzian dispersive time-varying media, *Appl. Phys. Lett.* **124**, 101701 (2024).
- [37] K.-H. Kim and K.-H. O, Graphene plasmonic time crystals, *Phys. Status Solidi* **18**, 2400116 (2024).
- [38] X. Wang, P. Garg, M. S. Mirmoosa, A. G. Lamprianidis, C. Rockstuhl, and V. S. Asadchy, Expanding momentum bandgaps in photonic time crystals through resonances, *Nat. Photonics* **19**, 149 (2025).
- [39] A. Salandrino, Plasmonic parametric resonance *Phys. Rev. B* **97**, 081401(R) (2018).
- [40] L. Bar-Hillel, Y. Plotnik, O. Segal, and M. Segev, Long lived surface plasmons on the interface of a metal and a photonic time-crystal, [arXiv:2412.10810](https://arxiv.org/abs/2412.10810) [Nanophotonics (to be published)].
- [41] V. P. Silin, Parametric resonance in a plasma, *Sov. Phys. JETP* **21**, 1127 (1965).
- [42] S. Zhang, J. Dong, H. Li, J. Xu, and B. Shapiro, Longitudinal optical phonons in photonic time crystals containing a stationary charge, *Phys. Rev. B* **110**, L100306 (2024).
- [43] W. Jaffray, S. Saha, V. M. Shalaev, A. Boltasseva, and M. Ferrera, Transparent conducting oxides: From all-dielectric plasmonics to a new paradigm in integrated photonics, *Adv. Opt. Photonics* **14**, 148 (2022).
- [44] N. Kinsey, C. DeVault, J. Kim, M. Ferrera, V. M. Shalaev, and A. Boltasseva, Epsilon-near-zero Al-doped ZnO for ultrafast switching at telecom wavelengths, *Optica* **2**, 616 (2015).
- [45] L. Caspani *et al.*, Enhanced nonlinear refractive index in ϵ -near-zero materials, *Phys. Rev. Lett.* **116**, 233901 (2016).
- [46] M. Z. Alam, I. De Leon, and R. W. Boyd, Large optical nonlinearity of indium tin oxide in its epsilon-near-zero region, *Science* **352**, 795 (2016).
- [47] Y. Zhou, M. Z. Alam, M. Karimi, J. Upham, O. Reshef, C. Liu, A. E. Willner, and R. W. Boyd, Broadband frequency translation through time refraction in an epsilon-near-zero material, *Nat. Commun.* **11**, 2180 (2020).
- [48] R. Tirole, S. Vezzoli, E. Galiffi, I. Robertson, D. Maurice, B. Tilmann, S. A. Maier, J. B. Pendry, and R. Sapienza, Double-slit time diffraction at optical frequencies, *Nat. Phys.* **19**, 999 (2023).
- [49] E. Lustig, O. Segal, S. Saha, E. Bordo, S. N. Chowdhury, Y. Sharabi, A. Fleischer, A. Boltasseva, O. Cohen, V. M. Shalaev, and M. Segev, Time-refraction optics with single cycle modulation, *Nanophotonics* **12**, 2221 (2023).
- [50] M. Silveirinha and N. Engheta, Tunneling of electromagnetic energy through sub-wavelength channels and bends using near-zero-epsilon materials, *Phys. Rev. Lett.* **97**, 157403 (2006).
- [51] N. Engheta, Pursuing near-zero response, *Science* **340**, 286 (2013).
- [52] R. Secondo, J. Khurgin, and N. Kinsey, Absorptive loss and band non-parabolicity as a physical origin of large non-linearity in epsilon-near-zero materials, *Opt. Mater. Express* **10**, 1545 (2020).
- [53] N. W. Ashcroft and N. D. Mermin, *Solid State Physics* (Holt, Reinhart and Winston, Philadelphia PA, 1976), Chap. 1.
- [54] C. Kittel, *Introduction to Solid State Physics*, 8th ed. (John Wiley and Sons, Hoboken NJ, 2005), Chap. 14.
- [55] See Supplemental Material <http://link.aps.org/supplemental/10.1103/PhysRevLett.134.183801> for a discussion of the following: I. Electromagnetic model for the time-modulated plasma. II. Summary of relevant results from Floquet theory. III. Parametric resonances at weak modulation. IV. Piecewise constant modulation. V. Numerical results for resonance growth rates for transverse modulated plasmons. This Supplemental Material also includes Ref. [56], which we include here for completeness.
- [56] E. M. Lifshitz and L. P. Pitaevskii, *Physical Kinetics*, The Landau and Lifshitz Course on Theoretical Physics Vol. X (Pergamon Press, Oxford, 1993), Sec. 28.
- [57] L. D. Landau and E. M. Lifshitz, *Mechanics*, 3rd ed. (Pergamon Press, Oxford, 1976), Sec. 27.
- [58] That is, up to a dimensionless coefficient which may depend, in general, on other dimensionless parameters in (2), such as the amplitude of the modulation depth $\delta_m(t)$.
- [59] The simplest ENZ material is perhaps ordinary dissipationless electron plasma with $\epsilon(\omega) = 1 - (\omega_p/\omega)^2$, with $\omega \approx \omega_p$.
- [60] L. Brillouin, *Wave Propagation in Periodic Structures—Electric Filters and Crystal Lattices* (McGraw Hill Book Company, New York, 1946), Chap. 8.
- [61] B. van der Pol and M. J. O. Strutt, On the stability of the solutions of Mathieu's equation, *Philos. Mag.* **5**, 18 (1928).
- [62] W. Magnus and S. Winkler, *Hill's Equation* (Dover Publications, New York, 2004).
- [63] F. M. Arscott, *Periodic Differential Equations* (The MacMillan Company, New York, 1964), Chap. 6; D. W. Jordan and P. Smith, *Nonlinear Ordinary Differential Equations*, 4th ed. (Oxford University Press, Oxford, 2007), Chap. 9.
- [64] I. Kiorpelidis, F. K. Diakonov, G. Theocharis, and V. Pagneux, Transient amplification in Floquet media: The Mathieu oscillator example, *Phys. Rev. B* **110**, 134315 (2024).
- [65] J. N. Winn, S. Fan, J. D. Joannopoulos, and E. P. Ippen, Interband transitions in photonic crystals, *Phys. Rev. B* **59**, 1551 (1999).